Pergamon

Tetrahedron 58 (2002) 6027–6032

TETRAHEDRON

Synthesis of rigid-rod linkers to anchor chromophores to semiconductor nanoparticles

Dong Wang, James M. Schlegel and Elena Galoppini*

Department of Chemistry, Rutgers University, 73 Warren Street, Newark, NJ 07102, USA

Received 16 April 2002; revised 3 June 2002; accepted 6 June 2002

Abstract—Four rigid-rod sensitizers, made of a phenylethynyl spacer substituted with a chromophore and two COOR binding groups, were prepared to study dynamics of electron injection at the interface of metal oxide semiconductor nanoparticles. Dimethyl Ru(bpy)$_2$(5-(5-1,10-phenanthrolinyl)ethynyl)isophthalate)$^{2+}$ (**4a**), dimethyl Ru(bpy)$_2$(5-(4-(2,2′-bipyridinyl)ethynyl)isophthalate)$^{2+}$ (**4b**), dimethyl 5-(1-pyrenylethynyl)isophthalate (**4c**), and dimethyl 5-(9-anthracenylethynyl)isophthalate (**4d**), were synthesized and characterized. Their absorption spectra, emission spectra, and electrochemical properties have been studied in acetonitrile and hexane solutions at room temperature. © 2002 Elsevier Science Ltd. All rights reserved.

1. Introduction

The functionalization of semiconductor and metal nanoparticles with chromophores and redox-active molecules is an important step toward the development of devices operating on the molecular level,[1,2] including solar cells, light-harvesting systems and chemical sensors.[1] Typically, their function is based on interfacial electron transfer processes. An important example is the light-to-energy conversion in photoelectrochemical solar cells by sensitization of nanocrystalline TiO$_2$ to visible light using Ru$^{\mathrm{II}}$-polypyridyl complexes.[3] The Ru$^{\mathrm{II}}$ sensitizers, typically Ru(dcb)(bpy)$_2^{2+}$,[4] are covalently attached to the TiO$_2$ nanoparticles through the carboxylic acid groups on the dcb ligand.[3,5] A recent area of interest in this field is the development of linkers that are rigid and that can distance the sensitizer from the nanoparticle surface, Scheme 1(a).[6,7] These are useful to study remote electron transfer processes and tune molecular–semiconductor interactions.[6,7] Analogous donor–spacer–acceptor systems have been successfully employed for decades to study electron transfer in fluid solutions[8] or at the surface of electrodes,[9] Scheme 1(b) and (c), respectively.

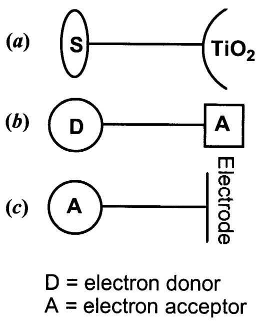

Scheme 1.

Recently, we have prepared tripod-shaped[10] linkers for metal oxide nanoparticles, such as **I** in Fig. 1.[11] These are 1,3,5,7-tetraphenyladamantane and tetraphenylmethane derivatives having three arms ending with COOR binding groups and the fourth arm carrying a phen or bpy-based Ru$^{\mathrm{II}}$-polypyridyl complex.[11] The three-point attachment and the structural rigidity of the molecule provide a high degree of control over the distance of the sensitizer from the metal oxide nanoparticles surface (~15 to 18 Å).[10,12] The study of the tripodal sensitizers prompted us to explore other types of linkers. Specifically, we were interested in ‘rigid-rods’,[9b,13] such as **II** in Fig. 1.

In the tripodal linkers, the saturated tetrahedral core (Td=sp^{3}C or adamantane) interrupts the conjugation between the sensitizer and the semiconductor surface, while the rigid rods are fully conjugated.[13] Second, rigid-rods have been successfully employed in SAM on gold.[9] When bound to nanocrystalline TiO$_2$ by the two COOR groups, linkers like **II** may enhance charge injection yields as the wavefunction is delocalized through the linker and possibly also enhance charge recombination rates to the chromophoric center.[9,13b] Furthermore, well-known cross-coupling methodologies[14] could allow to vary the number of phenyl and/or ethyne units between the tripod and the sensitizer and thereby the distance from the surface. In this paper we describe the synthesis, characterization and selected properties of the first examples of

---

Keywords: rigid-rod linkers; sensitization; semiconductor; nanoparticle.

* Corresponding author. Tel.: +1-973-353-5317; fax: +1-973-353-1264; e-mail: galoppin@andromeda.rutgers.edu

PII: S0040-4020(02)00586-0

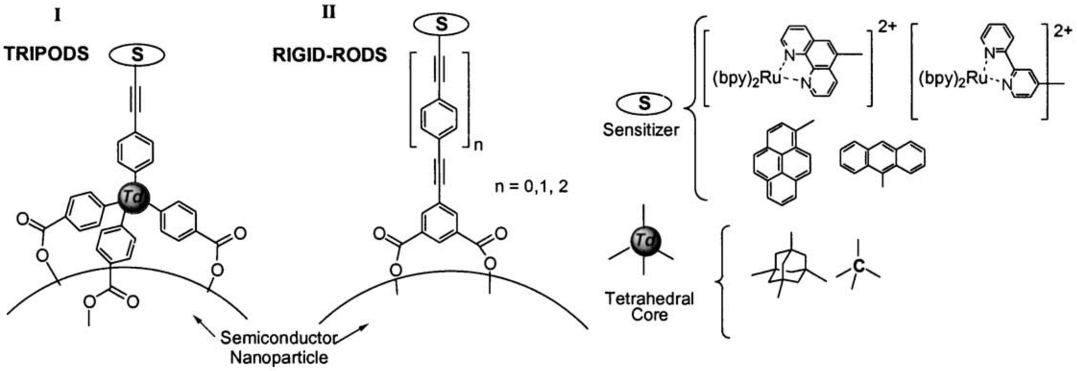

Figure 1. Representation of the two types of rigid sensitizers (tripods and rigid rods) and their components.

rigid-rod linkers **II** substituted with organic and inorganic sensitizers.

2. Results and discussion

Four rigid-rod sensitizers were prepared: **4a** and **b**, substituted with Ru^{II}-polypyridyl complexes, and **4c** and **d**, substituted with aromatic chromophores. Their synthesis is shown in Scheme 2.

Sonogashira cross-coupling[15] of dimethyl-5-bromo-isophthalate **1** with trimethylsilylacetylene, followed by deprotection with TBAF, produced alkyne **2**. Suzuki-type coupling[16] of **2** with 5-bromo-9,10-phenanthroline, 4-bromo-2,2′-bipyridine, 1-bromopyrene and 9-bromo-anthracene, yielded **3a**, **b**, **4c** and **d**, respectively. A Suzuki cross-coupling was employed in this step to avoid the dimerization of **2**, which is observed in Sonogashira coupling conditions. The compounds substituted with the phen and bpy ligands, **3a** and **b**, were easily converted into the corresponding Ru^{II} complexes **4a** and **b** by reaction with $Ru(bpy)_2Cl_2\cdot 2H_2O$. We found that the rigid-rods are considerably easier to synthesize and to purify than the tripodal sensitizers and are consistently obtained in good yields.

In addition to the Ru^{II}-polypyridyl complexes **4a** and **b**, that will be compared to the tripodal linkers, we prepared **4c** and **d**, substituted with pyrene and anthracene. It has been demonstrated that organic chromophores are frequently excellent test systems for elucidating fundamental photophysics of charge injection and recombination processes at molecule–nanoparticle interfaces.[17] In particular, anthracene directly bound to TiO_2 surfaces by a COOH group has been studied by others.[17b,c] Aromatic chromophores, with their well-defined spin states, vibronic structures and transition dipole orientations, can provide unique insights that are difficult to obtain from the more robust and widely used inorganic complex sensitizers. Although PL lifetimes of Ru^{II}–polypyridyl complexes are much longer ($\tau\sim1$ to 3 μs), the ultrafast electron injection rates observed in sensitizer–TiO_2 systems,[3] including those prepared from the tripodal sensitizers,[11a,b] are an assurance that the charge injection will be complete even with organic chromophores such as anthracene and pyrene. We expect that, even at the

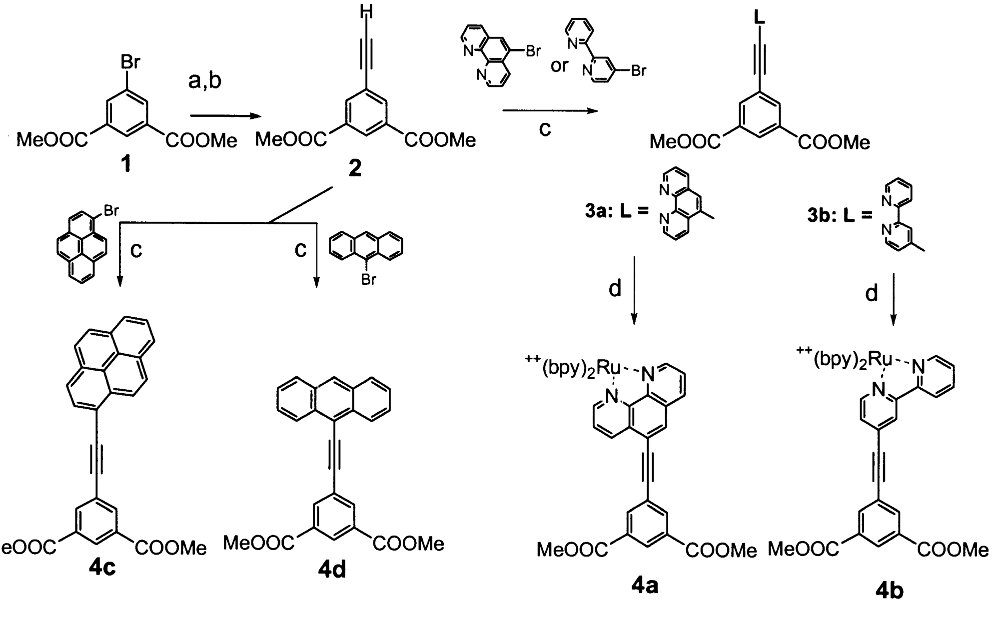

Scheme 2. *Reagents and yields*: (a) $Me_3SiC{\equiv}CH$, $Cl_2Pd(PPh_3)_2$, CuBr, $(i\text{-}Pr)_2NH$, reflux, 85%. (b) TBAF, THF, rt, 86%. (c) 1. $(Me_3Si)_2NLi$, −78°C; 2. 9-BBN, −78°C; 3. ArBr, $Pd(PPh_3)_4$, THF, reflux, 62–70%. (d) 1. $Ru(bpy)_2Cl_2\cdot 2H_2O$; 2. NH_4PF_6, 70%.

Table 1. Electrochemical and photophysical properties of rigid-rod sensitizers and reference sensitizers in solution

Compound	$E_{1/2\ \mathrm{ox}}$ (V)[a]	λ_{abs} (nm) (ε, M^{-1} cm^{-1})[b]	λ_{P} (nm)[c]	τ (μs)
4a	1.22[d]	451 (1.5×10^4)	610	1.79
Ru(phen)(bpy)$_2^{2+}$[e]	1.20[d,f]	450	620	1.20
4b	1.23[d]	462 (1.6×10^4)	640	3.20
Ru(bpy)$_3^{2+}$[e]	1.26,[d,g] 1.32[h]	452	626	0.80
4c[i]	1.20	383 (1.0×10^5)	428	0.060
Pyrene[i]	1.19	334 (7.5×10^4)	392	0.428
4d[i]	1.13	420 (1.0×10^4)	475	0.012
Anthracene[i]	1.19, 1.30[h]	375 (0.8×10^5)	421	0.015

[a] Half-wave potentials were measured at a Pt working electrode in 0.1 M TBAPF$_6$/CH$_3$CN degassed solution using Ag/AgCl as reference. Data are reported vs. SCE.

[b] Measurements were made at room temperature, absorption maximum ±2 nm.

[c] Photoluminescence maximum, ±4 nm. All data were obtained under argon atmosphere.

[d] Ru$^{\mathrm{III/II}}$.

[e] In CH$_3$CN.

[f] Ref. 19.

[g] Ref. 20.

[h] Ref. 21.

[i] In hexane.

increased distance, the charge injection into TiO$_2$ will be complete within the S$_1$ state lifetime of **4c** and **d** (60 and 12 ns, respectively, Table 1).

Selected properties of **4a–d** in fluid solutions and of reference chromophores (Ru(phen)(bpy)$_2^{2+}$, Ru(bpy)$_3^{2+}$, pyrene, and anthracene) are listed in Table 1. The oxidation waves for **4a–d** were similar to those of the references. Rigid-rod sensitizers **4a** and **b** displayed reversible Ru$^{\mathrm{III/II}}$ waves at ~1.22 V vs SCE and **4c** and **d** displayed oxidation waves at 1.20 and 1.13 V vs SCE. The visible absorption spectra of sensitizers **4a** and **b** in acetonitrile displayed broad bands typical of MLCT excited states. The phen-based **4a** and Ru(phen)(bpy)$_2^{2+}$ displayed the MLCT band centered at ~451 nm while the bpy-based **4b** displayed the MLCT ($\lambda_{\max}$=462 nm) red-shifted with respect to Ru(bpy)$_3^{2+}$, an observation that is consistent with data obtained for the tripodal sensitizers.[11a] The visible absorption spectra of **4c** and **d** displayed broad bands 49 and 45 nm red-shifted with respect to pyrene and anthracene,[18] respectively. All sensitizers displayed room-temperature photoluminescence (PL) and the emission maximum followed the same trends as the absorption. As expected, the PL decays of sensitizers **4a–d** in acetonitrile or hexane solutions followed single exponential kinetics.

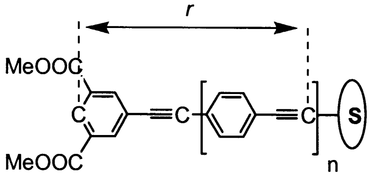

n	C to C r(Å)
0	5.4
1	12.2
2	19.1

Figure 2. Calculated C to C distances of rigid-rod linkers of various length (MM2, Spartan, Wavefunction, Inc.).

Finally, we are interested in increasing the number of phenylethynyl spacers, as shown in Fig. 2, and thereby control the distance between the semiconductor surface and the sensitizer. To test this possibility, we prepared linker **7** (**I** with n=1) through the route shown in Scheme 3. As in the case of shorter rods, linker **7** was a very soluble material. To avoid the dimerization of **6** in step (c), we employed coupling conditions different than those used in step (b).

3. Conclusions

Four sensitizers (**4a–d**) containing conjugated rigid-rod ligands were synthesized and characterized. Rigid spacers for sensitizers are useful models for photophysical and electron transfer studies at nanoparticle interfaces. The synthesis of linker **7**, containing two phenyethynyl units, demonstrates that the length of the spacer can be increased. The study of the binding properties to TiO$_2$ and other metal oxide nanoparticle surfaces, and the excited state and redox properties of surface-bound **4a–d** and sensitizers derived from **7** is in progress.

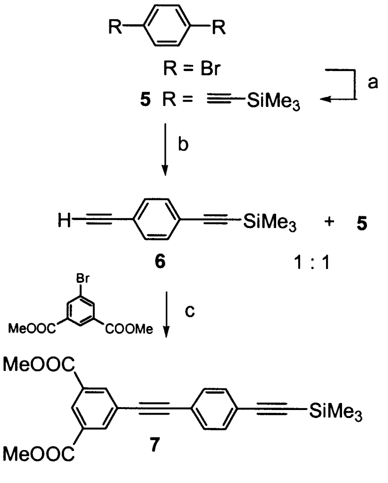

Scheme 3. *Reagents and yields*: (a) Me$_3$SiC≡CH, Cl$_2$Pd(PPh$_3$)$_2$, CuBr, (i-Pr)$_2$NH, reflux. 83%. (b) MeLi LiBr, THF, 0°C. (c) Pd(dba)$_2$, PPh$_3$, CuI, THF and Et$_3$N, reflux. 60%.

4. Experimental

4.1. Synthetic procedures

General. NMR spectra were obtained on a Varian INOVA 500 spectrometer operating at 499.90 MHz for ^{1}H and 124.98 MHz for ^{13}C and collected in $CDCl_3$, unless otherwise specified. The ^{1}H spectra were referenced to tetramethylsilane and the ^{13}C spectra to the central line of the solvent. Coupling constants (*J*) are reported in Hz with a precision of ±0.1 Hz. High- or low-resolution mass spectra (HRMS or LRMS) and elemental microanalytical data were obtained at commercial facilities (Michigan State University Mass Spectrometry Facility and Robertson Microlit Laboratories, Madison, NJ, respectively). GC/MS data were obtained on a HP 6890 gas chromatograph with a HP 5973 MS detector and a capillary column (HP 19091s-433: 30 m, phenylmethyl siloxane). Major ions are recorded to unit mass, intensity is parenthetically indicated as a percentage of the strongest peak. Melting points were measured with a Fisher melting point apparatus. UV–Vis absorption spectra were collected on a VARIAN Cary-500, and fluorescence emission spectra on a VARIAN Cary-Eclipse. IR measurements were made on a Mattson RS1 FT-IR spectrometer using polyethylene cards.

Materials. THF was purchased anhydrous (Aldrich) and then distilled first from sodium/benzophenone and then from $LiAlH_4$ immediately prior to use. Benzene was purchased anhydrous (Aldrich) or dried by removal of the water azeotrope followed by distillation from sodium. Et_3N and *i*-Pr_2NH were distilled from KOH under nitrogen prior to use. Spectroscopic grade CH_3CN for spectroscopic and electrochemical measurements was used without further purification. Organolithium reagents ($MeLi\cdot LiBr$ and $(Me_3Si)_2NLi$) and B-methoxy-9-borobicyclo[3,3,3]nonane (B-Methoxy-9-BBN) were purchased from Akros or from Aldrich. Column chromatography was performed using silica gel (Selecto Silica Gel, 230–600 mesh). TLC was performed on Whatman silica gel plates, using UV light as the developing agent. Dimethyl-5-bromoisophthalate is commercially available (Fluka) or can be easily prepared by treating the corresponding carboxylic acid with a solution of diazomethane in ether. Bis-1,4-(trimethylsilylethynyl)-benzene (**5**), which is commercially available, was prepared following the same procedure used to prepare **2**.

Methods. All reactions, except step (b) in Scheme 2, were performed under nitrogen atmosphere in glassware that had been oven-dried and flamed under vacuum and using anhydrous solvents. 'Standard workup' refers to extractions with the indicated organic solvent, followed by washing of the combined extracts with water or brine, drying over Na_2SO_4 and removal of solvents in vacuo on a rotary evaporator.

4.1.1. Dimethyl 5-ethynylisophthalate (2). To a solution of dimethyl-5-bromoisophthalate (140 mg, 0.51 mmol) in diisopropylamine (15 ml), were added $Cl_2Pd(PPh_3)_2$ (32 mg, 0.05 mmol), CuBr (110 mg, 0.53 mmol) and trimethylsilylacetylene (2 ml, or 1.4 g, 14 mmol). The reaction mixture was refluxed overnight, filtered and the solution was concentrated in vacuo. The solid residue was purified through silica gel column chromatography (hexane/ethyl acetate, 90:10) to give 125 mg of dimethyl 5-(trimethylsilylethynyl)isophthalate as a white solid (yield: 85%). Mp: 101–102°C. ^{1}H NMR δ: 8.61 (1H, s), 8.30 (2H, s), 3.95 (6H, s), 0.27 (9H, s). ^{13}C NMR δ: 165.58, 136.87, 130.84, 130.29, 124.24, 102.72, 96.74, 52.52, −0.20. GC/MS *m/z*: 290 (M^+, 15), 275 (M−15, 100), 259 (M−31, 10), 201 (M−89, 8). Tetrabutylammoniumfluoride trihydrate (160 mg, 0.52 mmol) was added to a THF solution of the TMS-protected alkyne (100 mg, 0.35 mmol). After stirring at room temperature for 2 h, was added water. After standard workup with chloroform, the crude product was purified through column chromatography (hexane/AcOEt, 90:10) to give 65 mg (yield: 86%) of **2** as a white solid. Mp: 124–125°C. ^{1}H NMR δ: 8.65 (1H, s), 8.33 (2H, s), 3.96 (1H, s), 3.18 (1H, s). ^{13}C NMR δ: 165.47, 137.07, 131.00, 130.69, 123.21, 81.56, 79.16, 52.58. GC/MS *m/z*: 218 (M^+, 60), 187 (M−31, 100), 159 (M−59, 35), 144 (M−74, 35), 100 (M−118, 15), 74 (M−144, 15). IR (cm^{-1}): 3250, 1728, 1594, 1270. Anal. Calcd for $C_{12}H_{10}O_4$: C, 66.05; H, 4.62; O, 29.33. Found: C, 65.85; H, 4.57.

4.2. Suzuki-type coupling of 2 with ArBr

In a typical procedure, to a solution of **2** (100 mg, 0.459 mmol) in THF (10 ml) at −78°C was added lithium bis(trimethylsilyl)amide (0.63 mmol, 0.63 ml of 1 M hexane solution). After 30 min, was added 9-methoxy-9-BBN (0.63 mmol, 0.63 ml of 1 M hexane solution). After stirring for 2 h at −78°C, the solution was transferred via cannula to a second flask containing $Pd(PPh_3)_4$ (31 mg, 0.028 mmol) and the aryl bromide (ArBr=0.386 mmol) in dry THF (15 ml). The reaction mixture was heated to reflux overnight and cooled to room temperature. After standard workup with chloroform the crude product was purified by silica gel column chromatography using the eluent indicated in each case.

4.2.1. 3a (ArBr=5-bromo-9,10-phenanthroline). Eluent: 1% of MeOH in $CHCl_3$. Yield: 68%. Mp: 160–161°C. ^{1}H NMR δ: 9.26 (1H, dd, J_1=4.0 Hz, J_2=2.0 Hz), 9.22 (1H, dd, J_1=4.0 Hz, J_2=2.0 Hz), 8.83 (1H, dd, J_1=8.0 Hz, J_2=1.5 Hz), 8.71 (1H, t, *J*=1.5 Hz), 8.51 (2H, d, *J*=1.5 Hz), 8.26 (1H, dd, J_1=8.0 Hz, J_2=1.5 Hz), 8.15 (1H, s), 7.79 (1H, dd, J_1=8.5 Hz, J_2=4.0 Hz), 7.68 (1H, dd, J_1=8.5 Hz, J_2=4.0 Hz), 4.01 (6H, s). ^{13}C NMR δ: 165.49, 151.23, 150.85, 146.34, 145.96, 136.60, 135.92, 134.59, 131.38, 131.22, 130.62, 128.08, 127.92, 123.72, 123.56, 123.53, 119.19, 93.09, 87.65, 52.66. MS *m/z*: 396 (M^+, 100), 365 (M−31, 10), 322 (M−74, 11), 277 (M−119, 10), 262 (M−134, 17), 183 (M−213, 15). HRMS (EI) calcd for $C_{24}H_{16}N_2O_4$: 396.1110, found 396.1114. IR (cm^{-1}): 1728, 1598, 1243.

4.2.2. 3b (ArBr=4-bromo-2,2′-bipyridine). Eluent: hexane/AcOEt, 80:20. Yield: 62%. Mp: 183–184°C. ^{1}H NMR δ: 8.71 (2H, m), 8.69 (1H, m), 8.58 (1H, s), 8.43 (1H, m), 8.41 (2H, d, *J*=1.5 Hz), 7.85 (1H, ddd, J_1=J_2=7.5 Hz, J_3=2.0 Hz), 7.42 (1H, dd, J_1=5.0 Hz, J_2=1.5 Hz), 7.35 (1H, ddd, J_1=7.5 Hz, J_2=4.5 Hz, J_3=1.0 Hz), 3.99 (6H, s). ^{13}C NMR δ: 165.43, 156.31, 155.29, 149.27, 137.11, 136.78, 131.67, 131.16, 130.90, 125.24, 124.15, 123.33, 121.21, 91.757, 88.67, 52.65. GC/MS *m/z*: 372 (M^+, 100), 341 (M−31, 42), 314 (M−58, 22), 298 (M−74, 11), 253 (M−119, 11), 170 (M−202, 16). Anal. Calcd for $C_{22}H_{16}N_2O_4$: C, 70.96; H, 4.33; N, 7.52; O, 17.19. Found: C, 70.65; H, 4.23; N, 7.20. IR (cm^{-1}): 1733, 1584, 1249.

4.2.3. 4c (ArBr=1-bromopyrene). Eluent: $CHCl_3$. Yield: 70%. Mp: 194–195°C. ^{1}H NMR *δ*: 8.67 (1H, t, *J*=1.5 Hz), 8.65 (1H, s), 8.53 (2H, d, *J*=1.5 Hz), 8.24 (4H, m), 8.14 (2H, m), 8.06 (2H, m), 4.01 (6H, s, COOC*H*$_3$). ^{13}C NMR *δ*: 165.69 (*C*OOCH$_3$), 136.50, 132.10, 131.69, 131.22, 131.07, 131.03, 130.07, 129.78, 128.68, 128.51, 127.21, 126.34, 125.86, 125.79, 125.34, 124.65, 124.55, 124.45, 124.26, 116.80, 92.95 (Pyr–C≡*C*–), 90.60 (Pyr–*C*≡C–), 52.61 (COO*C*H$_3$). HRMS (EI) calcd for $C_{28}H_{18}O_4$: 418.1205. Found: 418.1191. Anal. Calcd for $C_{28}H_{18}O_4$: C, 80.37; H, 4.34; O, 15.29. Found: C, 79.71; H, 4.30. IR (cm^{-1}): 2206, 1730, 1592, 1240.

4.2.4. 4d (ArBr=9-bromoanthracene). Eluent: $CHCl_3$. Yield: 66%. Mp: 231–232°C. ^{1}H NMR *δ*: 8.68 (1H, t, *J*=1.5 Hz), 8.64 (2H, d, *J*=8.5 Hz), 8.57 (2H, d, *J*=1.5 Hz), 8.48 (1H, s), 8.04 (2H, d, *J*=8 Hz), 7.65 (2H, ddd, J_1=8.5 Hz, J_2=6.5 Hz, J_3=1.0 Hz), 7.54 (2H, dd, J_1=8 Hz, J_2=6.5 Hz), 4.02 (6H, s, COOC*H*$_3$). ^{13}C NMR *δ*: 165.70 (*C*OOMe), 137.03, 136.42, 132.78, 131.10, 130.11, 128.77, 128.50, 126.99, 126.54, 125.80, 124.70, 116.20, 98.49 (An–C≡*C*), 88.25 (An–*C*≡C), 52.63 (COO*C*H$_3$). HRMS (EI) calcd for $C_{26}H_{18}O_4$: 394.1205. Found: 394.1200. Anal. Calcd for $C_{26}H_{18}O_4$: C, 79.17; H, 4.60; O, 16.23. Found: C, 79.39; H, 4.54. IR (cm^{-1}): 2196, 1728, 1595, 1246.

4.2.5. Formation of Ru^{II}–polypyridyl complexes. In a typical procedure, a solution of the ligand **3a** or **b** (0.311 mmol) in THF (3 ml) was added to a 1:1 mixture of ethanol/water (15 ml). To the solution, purged with nitrogen (15 min), was added $Ru(bpy)_2Cl_2\cdot 2H_2O$ (177 mg, 0.341 mmol) and the mixture was refluxed for 6 h, cooled to room temperature and filtered. Addition of aqueous NH_4PF_6 (3.0 g, 18.4 mmol) to the filtrate formed precipitate, which was collected and washed with water to afford the complex as an orange powder. **4a**: yield 70%. ^{1}H NMR *δ* (acetone-d$_6$): 9.26 (1H, d, *J*=3.0 Hz), 8.84 (7H, m), 8.63 (1H, t, *J*=2.0 Hz), 8.52 (3H, m), 8.27 (2H, m), 8.18 (4H, m), 8.05 (1H, m), 7.97 (3H, m), 7.65 (2H, m), 7.40 (2H, m), 3.99 (6H, s). ^{13}C NMR *δ* (acetone-d$_6$): 165.67, 158.40, 158.13, 154.37, 154.24, 153.08, 153.03, 148.72, 148.64, 139.09, 138.96, 137.77, 137.23, 136.46, 133.63, 132.56, 131.51, 131.48, 131.45, 128.77, 128.64, 127.89, 127.85, 125.36, 125.27, 124.01, 121.91, 95.80, 86.73, 53.10. Anal. Calcd for $C_{44}H_{32}F_{12}N_6O_4P_2Ru$: C, 48.05; H, 2.93; N, 7.64. Found: C, 46.70; H, 2.77; N, 7.26. IR (cm^{-1}): 1725, 1603, 1252, 841. **4b**: Yield 72%. ^{1}H NMR *δ* (acetone-d$_6$): 9.07 (1H, s), 8.95 (1H, d, *J*=3.0 Hz), 8.84 (4H, d, *J*=8.5 Hz), 8.63 (1H, t, *J*=1.5 Hz), 8.38 (1H, d, *J*=1.5 Hz), 8.22 (8H, m), 8.09 (4H, m), 7.72 (1H, dd, J_1=6 Hz, J_2=2 Hz), 7.61 (5H, m), 3.98 (6H, s). ^{13}C NMR *δ* (acetone-d$_6$): 165.53, 158.69, 158.10, 158.06, 157.99, 157.69, 152.95, 152.88, 152.81, 152.75, 152.64, 139.13, 139.05, 137.16, 132.63, 132.49, 131.79, 129.80, 129.14, 128.85, 127.19, 125.69, 129.39, 123.38, 95.68, 88.04, 53.15. Anal. Calcd for $C_{42}H_{32}F_{12}N_6O_4P_2Ru$: C, 46.89; H, 3.00; N, 7.81. Found: C, 46.16; H, 2.97; N, 7.44. IR (cm^{-1}): 1728, 1605, 1260, 840.

4.2.6. 1-Ethynyl-4-(trimethylsilylethynyl)benzene (6). To a solution of **5** (800 mg, 2.96 mmol) in THF (30 ml) cooled with an water/ice bath, MeLi·LiBr (2.97 mmol, 1.35 ml of 2.2 M solution in diethyl ether) was added dropwise (~20 min). The solution was stirred for 10 min and then poured into ice-cold, diluted HCl aq. After standard workup with ether were obtained 540 mg of a ~1:1 mixture of **5** and **6** (GC/MS). This mixture was difficult to separate and it was used in the next step after purification through a short pad of silica gel. A small amount of **6** was isolated by silica gel column chromatography (pentane) for characterization purposes: ^{1}H NMR *δ*: 7.39 (4H, s), 3.14 (1H, s, C≡C*H*), 0.23 (9H, s, Si(C*H*$_3$)$_3$). ^{13}C NMR *δ*: 131.90, 131.81, 123.57, 122.08, 104.33 (*C*≡CSi), 96.46 (C≡*C*Si), 83.19 (*C*≡CH), 78.92 (C≡*C*H), −0.12 (Si(*C*H$_3$)$_3$). GC/MS *m/z*: 198 (M$^+$, 30), 183 (M−15, 100), 28 (M−170, 30).

4.2.7. Synthesis of 7. To a solution of a mixture of **5** and **6** (amount of **6** estimated by GC/MS is 396 mg, 2.00 mmol), dimethyl 5-bromoisophthalate (273 mg, 1.00 mmol), bis(dibenzylideneacetone)palladium (30 mg, 0.05 mmol), PPh_3 (52 mg, 0.20 mmol), CuI (19 mg, 0.10 mmol) were added dry THF (20 ml) and Et_3N (147 mg, 1.50 mmol). The reaction mixture was refluxed for 24 h. The solvent was removed in vacuo and the crude product was purified by silica gel column chromatography (hexane/AcOEt, 95:5) to give 233 mg of **7** as a pale yellow powder (yield: 60% calculated on **1**). Mp: 161–162°C. ^{1}H NMR *δ*: 8.63 (1H, t, *J*=1.5 Hz), 8.35 (2H, d, *J*=1.5 Hz), 7.47 (4H, m), 3.97 (6H, s, COOC*H*$_3$), 0.26 (9H, s, Si(C*H*$_3$)$_3$). ^{13}C NMR *δ*: 165.56 (*C*OOMe), 136.48, 131.97, 131.52, 131.00, 130.20, 124.13, 123.57, 122.45, 104.42, 96.71, 90.84, 89.13, 52.55 (COO*C*H$_3$), −0.11 (Si(*C*H$_3$)$_3$). GC/MS *m/z*: 390 (M$^+$, 70), 375 (M−15, 100), 172 (M−218, 15). HRMS (EI) calcd for $C_{23}H_{22}O_4Si$: 390.1287, found 390.1289. IR (cm^{-1}): 2157, 1730, 1597, 1244.

4.3. Spectroscopic measurements

UV–Vis absorbance. UV–Vis absorbance measurements were made on a VARIAN Cary-500 spectrophotometer, using hexane as solvent for pyrene, anthracene, **4c** and **4d** and acetonitrile for **4a** and **4b**. The measurements were performed in 1 cm^2 cuvettes with following set-up parameters: 0.5 nm of data interval, 0.6 s of average time and 1.0 nm of SBW.

Photoluminescence. Photoluminescence (PL) spectra were obtained with a VARIAN Cary-Eclipse Fluorescence Spectrophotometer using hexane as solvent for pyrene, anthracene, **4c** and **d** and acetonitrile for **4a** and **b** in 4-way transparent 1 cm^2 cuvettes. The excitation slit was 5 nm and emission slit was 1.5 nm. The excitation wavelengths for pyrene, anthracene, **4a–d** are 305, 323, 450, 465, 360 and 395 nm, respectively. The PMT detector voltage was 800 V.

Time-resolved photoluminescence. Time-resolved photoluminescence decays were acquired on a nanosecond Nd:YAG (Continuum NY-61) laser. Measurements were acquired using 355 nm laser pulse for solutions of pyrene, anthracene, **4c** and **d** in hexane and 532 nm laser pulse for solutions of **4a** and **b** in acetonitrile, ca. 8 ns, 30–50 mJ. Samples were degassed by three freeze–pump–thaw cycles.

The samples concentrations were such that $A\sim0.3$ at the corresponding excitation wavelength. Each kinetic trace was acquired averaging 16 laser shots.

Electrochemistry. Cyclic voltammetry was performed in 0.1 M tetrabutylammonium hexafluorophosphate acetonitrile ($TBAPF_6/CH_3CN$) degassed solutions with scan rate=100 mV/s. The solutions were ~0.1 mM in the sensitizers. A BAS model CV-50 W potentiostat was used in a standard three-electrode arrangement consisting of a Pt working electrode, a Pt wire auxiliary counter electrode, and Ag/AgCl as the reference electrode. The measurements were carried out under nitrogen atmosphere and at room temperature and were recorded in the absence and in the presence of ferrocene. All half-wave potentials are referenced to the ferrocene/ferrocenium couple and are reported vs SCE.

Acknowledgements

E. G. and D. W. thank Professor Piotr Piotrowiak for help with the spectroscopic measurements and for insightful discussions. The Division of Chemical Sciences, Office of Basic Energy Sciences, Office of Science, US Department of Energy and the Petroleum Research Fund (ACS-PRF 35081-G5) are gratefully acknowledged for research support.

References

1. (a) *Molecular Electronics*; Jortner, J., Ratner, M., Eds.; Blackwell: London, 1997. (b) Meyer, G. J. *Molecular Level Artificial Photosynthetic Materials; Progress in Inorganic Chemistry*; Wiley: New York, 1997.
2. Alivisatos, A. P. *J. Phys. Chem.* **1996**, *100*, 13226.
3. (a) Hagfeldt, A.; Grätzel, M. *Chem. Rev.* **1995**, *95*, 49. (b) Kamat, P. V. *Chem. Rev.* **1993**, *93*, 267. (c) O'Regan, B.; Grätzel, M. *Nature* **1991**, *353*, 737. (d) Grätzel, M. *Heterogeneous Photochemical Electron Transfer*; CRC: Boca Raton, Florida, 1989. (e) Gerischer, H. *Photochem. Photobiol.* **1972**, *16*, 243.
4. Abbreviations used in this paper: dcb=4,4′-$(COOH)_2$-2,2′-bipyridine; bpy=2,2′-bipyridine; phen=1,10-phenanthroline.
5. Depending on the surface treatment and the binding conditions, the carboxylic groups bind covalently to the surface by reacting with surface OH groups and forming ester bonds, or can form carboxylates that interact with the surface in an unknown manner. The binding mode is usually determined by IR (C=O stretching). The ester linkages provide strong electronic coupling between the complex and the semiconductor and are thought to cause the ultrafast (femtosecond) electron injection rate constants that have been measured.
6. Meyer, G. J. *J. Chem. Ed.* **1997**, *74*, 652.
7. (a) Heimer, T. A.; D'Arcangelis, S. T.; Farzad, F.; Stipkala, J. M.; Meyer, G. J. *Inorg. Chem.* **1996**, *35*, 5319. (b) Asbury, J. B.; Hao, E.; Wang, Y.; Lian, T. *J. Phys. Chem. B* **2000**, *104*, 11957.
8. (a) Piotrowiak, P. *Chem. Soc. Rev.* **1999**, *28*, 143 and references therein. (b) Closs, G. L.; Johnson, M. D.; Miller, J. R.; Piotrowiak, P. *J. Am. Chem. Soc.* **1989**, *111*, 3751. (c) Closs, G. L.; Calcaterra, L. T.; Green, N. J.; Penfield, K. W.; Miller, J. R. *J. Phys. Chem.* **1986**, *90*, 3673.
9. (a) Bakkers, E. P. A. M.; Roest, A. L.; Marsman, A. W.; Jenneskens, L. W.; de Jong-van Steensel, L. I.; Kelly, J. J.; Vanmaekelbergh, D. *J. Phys. Chem. B* **2000**, *104*, 7266 and references therein. (b) Yang, G. H.; Qian, Y. L.; Engtrakul, C.; Sita, L. R.; Liu, G. Y. *J. Phys. Chem. B* **2000**, *104*, 9059. (c) Roncali, J. *Acc. Chem. Res.* **2000**, *33*, 147. (d) Vondrak, T.; Wang, H.; Winget, P.; Cramer, C. J.; Zhu, X. Y. *J. Am. Chem. Soc.* **2000**, *122*, 4700.
10. Tripod-shaped linkers of various structure (also named caltrops, see Ref. 9c) have been previously reported in studies of redox active molecules bound on gold electrodes: (a) Hirayama, D.; Takimiya, K.; Aso, Y.; Otsubo, T.; Hasobe, T.; Yamada, H.; Imahori, H.; Fukuzumi, S.; Sakata, Y. *J. Am. Chem. Soc.* **2002**, *124*, 532. (b) Yao, Y.; Tour, J. M. *J. Org. Chem.* **1999**, *64*, 1968. (c) Fox, M. A.; Whitesell, J. K.; McKerrow, A. *J. Langmuir* **1998**, *14*, 816. (d) Hu, J.; Mattern, L. *J. Org. Chem.* **2000**, *65*, 2277. For tetrahedral molecules with extended arms see: (e) Aujard, I.; Baltaze, J.-P.; Baudin, J.-B.; Cogné, E.; Ferrage, F.; Jullien, L.; Perez, E.; Prévost, V.; Qian, L. M.; Ruel, O. *J. Am. Chem. Soc.* **2001**, *123*, 8177.
11. (a) Galoppini, E.; Guo, W.; Zhang, W.; Hoertz, P.; Qu, P.; Meyer, G. J. *J. Am. Chem. Soc.* **2002** in press. (b) Galoppini, E.; Guo, W.; Qu, P.; Meyer, G. J. *J. Am. Chem. Soc.* **2001**, *123*, 4342. (c) Guo, W.; Galoppini, E.; Rydja, G. I.; Pardi, G. *Tetrahedron Lett.* **2000**, *41*, 7419.
12. This is defined as the distance from the Ru center to the footprint, i.e. the plane defined by the three surface-bound oxygen atoms.
13. For conjugated linkers used to attach redox-active molecules on gold see for instance (a) Sikes, H. D.; Smalley, J. F.; Dudek, S. P.; Cook, A. C.; Newton, M. D.; Chidsey, C. E. D.; Feldberg, S. W. *Science* **2001**, *291*, 1519. (b) Davis, W. B.; Svec, W. A.; Ratner, M. A.; Wasielewski, M. R. *Nature* **1998**, *396*, 60.
14. (a) Coupling Reactions Between sp Carbon Centers. *Comprehensive Organic Synthesis*; Sonogashira, K., Ed.; Pergamon: Oxford, 1991; Vol. 3, pp 551–561, Chapter 25. (b) *Metal-Catalyzed Cross-Coupling Reactions*; Stang, P. J., Diederich, F., Eds.; Wiley-VCH: Weinheim, 1998. (c) *Modern Acetylene Chemistry*; Stang, P. J., Diederich, F., Eds.; Wiley-VCH: Weinheim, 1995. (d) Bunz, U. H. F. *Synlett* **1997**, 1117.
15. Sonogashira, K. *Comprehensive Organic Synthesis*; Trost, B. M., Ed.; Pergamon Press: Oxford, 1991; Vol. 3, p 551.
16. (a) Soderquist, T. A.; Matos, K.; Rane, A.; Ramos, J. *Tetrahedron Lett.* **1995**, *36*, 2401. (b) Miyaura, N.; Suzuki, A. *Chem. Rev.* **1995**, *95*, 2457. (c) Brown, H. C.; Bhat, N. G.; Srebnik, M. *Tetrahedron Lett.* **1988**, *29*, 2631.
17. (a) Ramakrishna, S.; Willig, F. *J. Phys. Chem. B* **2000**, *104*, 68. (b) Martini, I.; Hodak, J. H.; Hartland, G. V. *J. Phys. Chem. B* **1998**, *102*, 9508. (c) Martini, I.; Hodak, J. H.; Hartland, G. V.; Kamat, P. V. *J. Chem. Phys.* **1997**, *107*, 8064. (d) Hannappel, T.; Burfeindt, B.; Storck, W.; Willig, F. *J. Phys. Chem. B* **1997**, *101*, 6799. (e) Ramakrishna, G.; Ghosh, H. N. *J. Phys. Chem. B* **2001**, *105*, 7000.
18. The data for pyrene and antracene in Table 1 were determined experimentally and are close to values reported in literature: Murov, S. L.; Carmichael, I.; Hug, G. L. *Handbook of Photochemistry*; Marcel Dekker: New York, 1993.
19. Vlcek, A. A.; Dodsworth, E. S.; Pietro, W. J.; Lever, A. B. P. *Inorganic Chemistry* **1995**, *34*, 1906.
20. Bugnon, P.; Hester, R. E. *Chem. Phys. Lett.* **1983**, *102*, 537.
21. *Electrochemical Methods*; Bard, A. J., Faulkner, L. R., Eds.; Wiley: New York, 2001; p 811.